The official journal of
INTERNATIONAL FEDERATION OF PIGMENT CELL SOCIETIES · SOCIETY FOR MELANOMA RESEARCH
PIGMENT CELL & MELANOMA Research

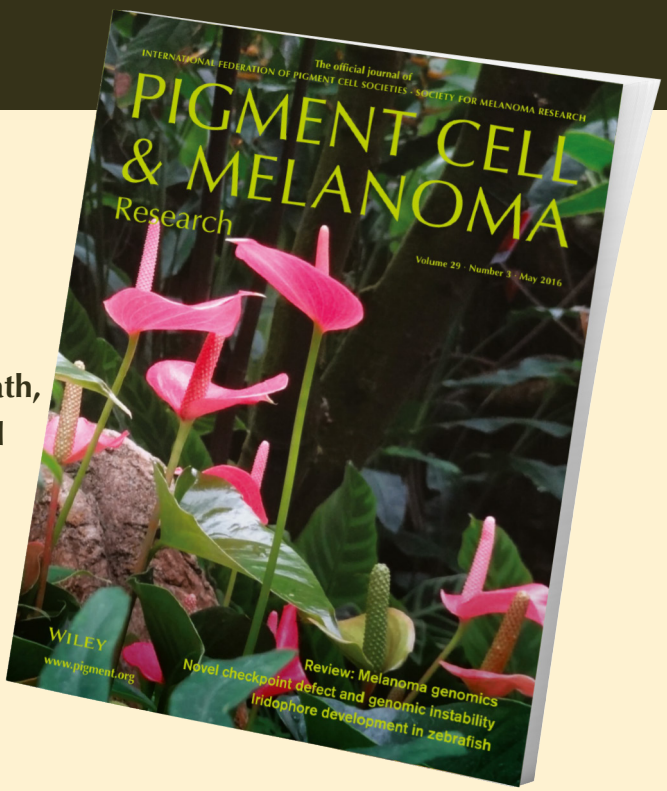

A novel ATM-dependent checkpoint defect distinct from loss of function mutation promotes genomic instability in melanoma

Loredana Spoerri, Kelly Brooks, KeeMing Chia, Gavriel Grossman, Jonathan J. Ellis, Mareike Dahmer-Heath, Dubravka Škalamera, Sandra Pavey, Bryan Burmeister and Brian Gabrielli

DOI: 10.1111/pcmr.12466
Volume 29, Issue 3, Pages 329–339

A novel ATM-dependent checkpoint defect distinct from loss of function mutation promotes genomic instability in melanoma

Loredana Spoerri[1,†], Kelly Brooks[1,*,†], KeeMing Chia[1,2], Gavriel Grossman[1], Jonathan J. Ellis[1], Mareike Dahmer-Heath[1], Dubravka Škalamera[1], Sandra Pavey[1], Bryan Burmeister[1,3] and Brian Gabrielli[1]

1 The University of Queensland Diamantina Institute, The University of Queensland, Brisbane, Qld, Australia **2** The Kinghorn Cancer Centre, Garvan Institute of Medical Research, Sydney, NSW, Australia **3** Division of Cancer Services, Princess Alexandra Hospital, Brisbane, Qld, Australia *Current address: Cancer Research UK Manchester Institute, The University of Manchester, Wilmslow Road, Manchester, M20 4BX, UK

CORRESPONDENCE Brian Gabrielli, e-mail: briang@uq.edu.au

[†]Equal contribution from these two authors.

KEYWORDS melanoma/ATM/checkpoint arrest/PLK1/genomic instability

PUBLICATION DATA Received 23 December 2015, revised and accepted for publication 3 February 2016, published online 8 February 2016

doi: 10.1111/pcmr.12466

Summary

Melanomas have high levels of genomic instability that can contribute to poor disease prognosis. Here, we report a novel defect of the ATM-dependent cell cycle checkpoint in melanoma cell lines that promotes genomic instability. In defective cells, ATM signalling to CHK2 is intact, but the cells are unable to maintain the cell cycle arrest due to elevated PLK1 driving recovery from the arrest. Reducing PLK1 activity recovered the ATM-dependent checkpoint arrest, and over-expressing PLK1 was sufficient to overcome the checkpoint arrest and increase genomic instability. Loss of the ATM-dependent checkpoint did not affect sensitivity to ionizing radiation demonstrating that this defect is distinct from ATM loss of function mutations. The checkpoint defective melanoma cell lines over-express PLK1, and a significant proportion of melanomas have high levels of PLK1 over-expression suggesting this defect is a common feature of melanomas. The inability of ATM to impose a cell cycle arrest in response to DNA damage increases genomic instability. This work also suggests that the ATM-dependent checkpoint arrest is likely to be defective in a higher proportion of cancers than previously expected.

Introduction

Genomic instability is a common feature of melanoma, and the degree of genomic instability can influence disease prognosis (Kaufmann et al., 2014). However, the defective mechanisms that promote this genomic instability are still poorly understood. Cell cycle checkpoints are stress-response mechanisms that prevent propagation of damaged DNA by pausing the cell cycle and promoting repair of the DNA lesions when the damage is manageable. Defects in cell cycle checkpoints, usually loss of function mutations in key components such as p53 and BRCA1, are a common feature of cancers (Medema and Macurek, 2012). Mutation and loss of function of key cell cycle checkpoint regulators CDKN2A/p16 and p53 are present in more than 50% of melanomas, and other genes with roles in cell cycle regulation and responses to DNA damage are also common targets for mutation (Hill et al., 2013; Lu et al., 2014). Thus loss of normal cell cycle checkpoint responses is likely to be significant contributors to genomic instability in melanoma.

Significance

Melanomas have high levels of genomic instability that can contribute to poor disease prognosis. The identification of this novel defect in a major response mechanism to DNA damage and the demonstration that it allows for survival with increased DNA damage, provides new insights into the defects that promote genomic instability in melanoma.

Cell cycle checkpoint defects are a relatively common feature of melanoma (Kaufmann et al., 2008; Wigan et al., 2012). We have previously reported that the G2 phase Topoisomerase II inhibitor-triggered decatenation checkpoint is common defective in melanoma cell lines (Brooks et al., 2013a). TopoII inhibitors trigger an Ataxia Telangiectasia Mutated (ATM)-dependent G2 phase arrest through direct recruitment of MDC1 to the chromatin (Luo et al., 2009). In the presence of the catalytic TopoII inhibitor ICRF-193, the checkpoint defective melanoma cell lines fail to arrest in G2 phase and progress through an aberrant mitosis resulting in the asymmetrical partitioning of the genome, potentially contributing to genetic instability (Brooks et al., 2013a). ATM mutations are rare in melanoma, and proteins implicated in decatenation checkpoint function including TOP2A, TOP2B, ATR, BRCA1 and WRN appeared normal in the checkpoint defective melanomas (Brooks et al., 2013a), thus the underlying mechanism that facilitates this checkpoint defect is at present unknown. Defective decatenation checkpoint responses have also been reported in other cancer types, although the molecular basis for these defects was not reported (Doherty et al., 2003; Nakagawa et al., 2004).

Decatenation checkpoint signalling is dependent on ATM and Polo-like kinase 1 (PLK1) (Bower et al., 2010; Deming et al., 2002; Luo et al., 2009). ATM also responds to DNA double strand breaks (DSBs) by phosphorylating and activating histone H2AX, MDC1, 53BP1, BRCA1 and ultimately CHK2 (Lobrich and Jeggo, 2007). The activation of CHK2 blocks CDC25B activation of Cyclin B/CDK1 thereby preventing entry into mitosis (Bartek et al., 2004; Boutros et al., 2006). PLK1 also plays a role in cell cycle checkpoint regulation via its roles in promoting G2/M phase transition and in mitosis (Macurek et al., 2008; Seki et al., 2008), with PLK1 activation blocked by ATM-CHK2 signalling (Smits et al., 2000; Tsvetkov and Stern, 2005). PLK1 has also been reported to have a role in recovery from G2 phase checkpoint arrest (Van Vugt et al., 2004).

This study investigates the molecular mechanisms underlying the ATM-dependent decatenation checkpoint defect common in melanoma cell lines (Brooks et al., 2013a). We have identified a novel cell cycle checkpoint defect characterized by intact ATM-CHK2 activation. This checkpoint signalling is unable to maintain a stable checkpoint arrest, destabilized by elevated PLK1. Inhibition of PLK1 was sufficient to recover the ATM-dependent checkpoint arrest, and over expression of PLK1 was sufficient to overcome the ATM-dependent arrest to promote genomic instability.

Results

Melanoma cells have defective ATM-dependent checkpoint arrest

ATM kinase has been shown to signal the TopoII inhibitor-sensitive decatenation checkpoint arrest (Bower et al., 2010; #2). We reasoned that in the decatenation checkpoint defective cells, the checkpoint arrest in response to DNA damaging agents that promote DSBs and signal a G2 phase checkpoint arrest through ATM-CHK2 may also be impaired. Time lapse imaging of a panel of decatenation checkpoint functional and defective cell lines treated with etoposide, a TopoII poison that produces DSBs, produced a stable G2 phase arrest in decatenation checkpoint functional cell lines, demonstrated by the complete block of progression into mitosis in these cell lines. In contrast, decatenation checkpoint defective cell lines had attenuated arrests and continued to progress into mitosis, albeit at a slower rate than the control or ICRF-193-treated cells (Figure 1A, B). A similar attenuated cell cycle arrest was also observed in decatenation checkpoint defective melanoma cell lines treated with phleomycin, a radiomimetic drug (Figure S1A). The delayed entry into mitosis observed in the checkpoint defective cell lines was the result of activation of CHK1 (phospho-CHK1 Ser317) with the DSB agents (Figure S1B), whereas CHK1 was not activated with ICRF-193 (Figure S1B). Inhibition of CHK1 activity using the selective inhibitor GNE-323 completely overcame the attenuated G2 phase delay in the checkpoint defective cell lines, but only partially attenuated the delay in the checkpoint functional A2058 cell line (Figure 1C). Ionizing radiation also produced a sustained block of progression into mitosis in a checkpoint functional cell line, indicated by the loss of the mitotic marker pMEK1 Thr286, and an attenuated response in a checkpoint defective cell line, with full recovery of the mitotic marker by 6–8 after irradiation. The ATM mutant HT144 cells were unaffected by radiation treatment as expected (Figure S1C). Thus, the lack of ATM-dependent checkpoint arrest in response to ICRF-193 was also found with agents that trigger ATM through DSBs.

ATM-CHK2 activation is intact in checkpoint defective cells

The activation of ATM and CHK2 in response to ICRF-193, etoposide and phleomycin was examined. Surprisingly, ATM and CHK2 activation was not only observed in checkpoint functional but also in defective cells in response to each drug (Figure 2A, B). Although the degree of activation was cell line dependent, the range of activation was similar in the checkpoint functional and defective lines analysed. The higher level of activation observed with phleomycin in all cell lines reflects the drug's ability to cause DSBs independent of the cell cycle, whereas the TopoII targeted drugs predominantly affect G2 phase cells when TopoII is most active. An increased basal level of ATM and CHK2 activation was also observed in the checkpoint defective cell lines. There was a significant trend for increased pCHK2 (Figure S2A, B), but not pATM (Figure S2C, D), in the checkpoint defective melanoma cell lines, an indicator of the increased replicative stress previously reported in these

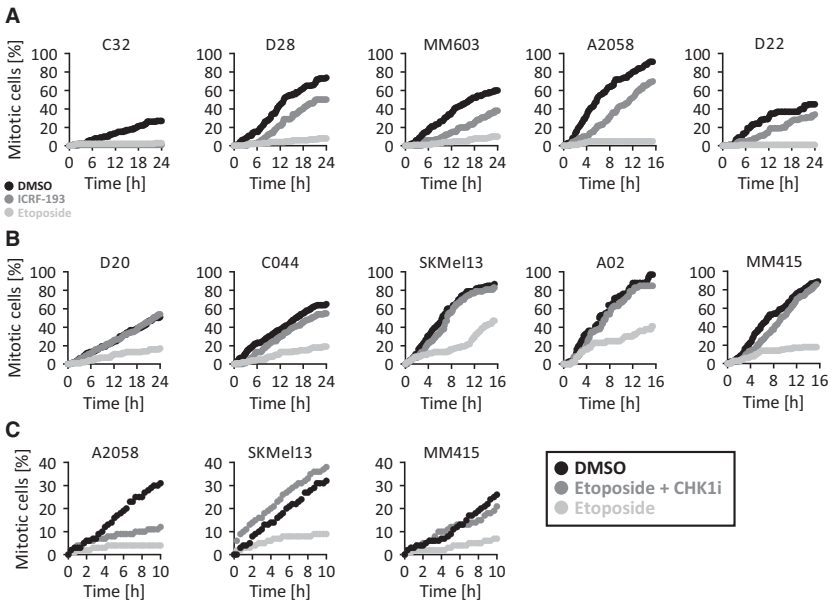

Figure 1. Decatenation checkpoint defective cell lines have an impaired checkpoint arrest in response to DNA double strand breaks (DSBs). (A) Five checkpoint-functional and (B) five checkpoint-defective cell lines were incubated with 2 μM ICRF-193, 2 μM etoposide or DMSO and the cell rate of entry into mitosis assessed by time-lapse microscopy over a period of 16 or 24 h (intervals = 10 min). (C) Checkpoint-functional A2058, and checkpoint-defective SKMel13 and MM415 were treated with either DMSO, 2 μM etoposide without and with 1 μM CHK1 inhibitor GNE-323 (CHK1i) and followed by time-lapse microscopy as above.

lines (Brooks et al., 2013a). The activation of ATM and CHK2 occurred with similar kinetics in the checkpoint functional and defective cells (Figure 2C, D), although the degree of activation in the checkpoint defective D20 lines was lower, reflecting the elevated basal CHK2 activation in the line (FigureS2A, E). Similarly with ionizing radiation induced DNA damage, the kinetic of activation of CHK1 and CHK2 were indistinguishable between the checkpoint functional and defective cell lines (Figure S2F).

ATM checkpoint signalling is initiated at the sites of DNA damage, where ATM co-localizes with DNA damage sensing, signalling and repair proteins (Bekker-Jensen et al., 2006). Nuclear foci of co-localized pATM, γH2AX and 53BP1 were found in both decatenation checkpoint functional (A2058 and D22) and defective (SKMel13 and MM415) cell lines with all drug treatments used (Figure 2E, F and Figure S3A–D). This indicated that normal ATM-dependent checkpoint signalling complexes were being assembled, and that ATM-dependent signalling was functional. Together, these data demonstrate that the loss of checkpoint arrest was not a consequence of defective ATM signalling.

The ATM target p53 was also examined. While p53 mutations were more common in the checkpoint defective lines, analysis of p53 activity (p53 Ser15 phosphorylation, p53 accumulation, increased p21 expression) in a subset of lines showed it was not commonly activate in either checkpoint functional or defective cell lines in response to ICRF193 treatment (Table S1). This suggested that p53 had little involvement in responses to ICRF193.

One feature of ATM mutant cells is their sensitivity to ionizing radiation induced DNA damage. However, there was little difference in the sensitivity of checkpoint functional and defective cell lines to ionizing radiation, whereas the ATM mutant HT144 cells were hypersensitive had a complete loss of viability with low dose (2.4 Gy) exposure (Figure 3). The sensitivity to ionizing radiation was increased by inhibiting ATM with the small molecule inhibitor KU55933 in all cell lines.

PLK1 level and activity are upregulated in checkpoint defective cell lines

The intact ATM signalling found in the checkpoint defective cell lines suggested that other components of the ATM checkpoint signalling pathway may be defective. The expression of a panel of ATM checkpoint signalling components including ATM, CHK2, RAD50, TP53BP1, MDC1, MRE11A, RAD51, NBS1, FANCD2, H2AFX, TOPBP1, TOP2A, TOP2B, BRCA1, WRN and PLK1 was assessed in a panel of melanoma cell lines using gene expression data previously generated for these cell lines (Johansson et al., 2007). Only PLK1 showed a consistent class effect, with significantly increased (1.8 fold) expression in the checkpoint defective cell lines (Figure 4A). Previous analysis of this data set identified PLK1 as being significantly downregulated ($P > 0.01$) in the checkpoint defective cell lines (Brooks et al., 2013a). PLK1 has a critical role in G2 phase checkpoint arrest and in recovery from the G2 phase checkpoint arrest (Van Vugt et al., 2004). This suggested the elevated PLK1 might effectively be over-riding the ATM-dependent G2 phase checkpoint arrest by promoting the normal checkpoint recovery mechanism. PLK1 protein levels were also significantly higher (~1.5 fold) in the checkpoint defective cell lines compared to the checkpoint functional cell lines, consistent with the gene expression data. The level of activated PLK1 (pPLK1) was also significantly higher in checkpoint defective cell lines (Figure 4B, C). High content imaging also demonstrated increased level of

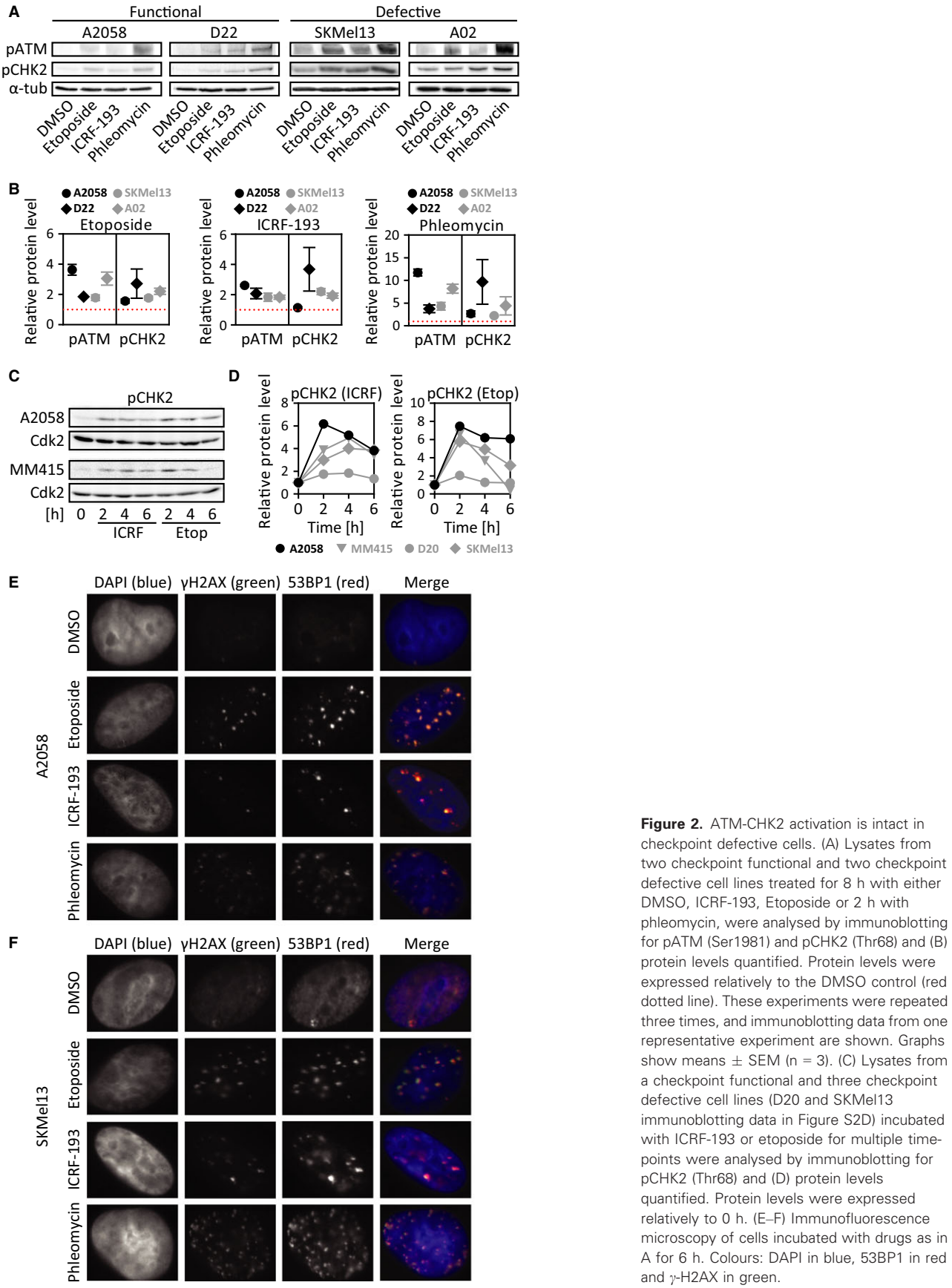

Figure 2. ATM-CHK2 activation is intact in checkpoint defective cells. (A) Lysates from two checkpoint functional and two checkpoint defective cell lines treated for 8 h with either DMSO, ICRF-193, Etoposide or 2 h with phleomycin, were analysed by immunoblotting for pATM (Ser1981) and pCHK2 (Thr68) and (B) protein levels quantified. Protein levels were expressed relatively to the DMSO control (red dotted line). These experiments were repeated three times, and immunoblotting data from one representative experiment are shown. Graphs show means ± SEM (n = 3). (C) Lysates from a checkpoint functional and three checkpoint defective cell lines (D20 and SKMel13 immunoblotting data in Figure S2D) incubated with ICRF-193 or etoposide for multiple time-points were analysed by immunoblotting for pCHK2 (Thr68) and (D) protein levels quantified. Protein levels were expressed relatively to 0 h. (E–F) Immunofluorescence microscopy of cells incubated with drugs as in A for 6 h. Colours: DAPI in blue, 53BP1 in red and γ-H2AX in green.

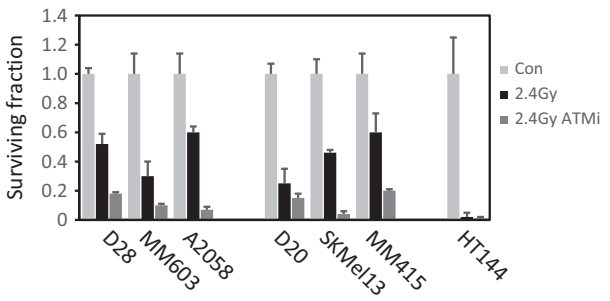

Figure 3. Checkpoint defective cell lines are not hypersensitive to Ionizing radiation. Checkpoint functional and effective cell lines, and the ATM mutant HT144 cell line were irradiated with 2.4 Gy ionizing radiation then treated without and with 10 μM ATM inhibitor (ATMi) KU55933 for 24 h, then replated at 400 cell per plate. Colonies were allowed to form for 2 weeks, then the cells were fixed and stained with Crystal Violet and the colonies per plate counted. The data are the mean and standard deviation from triplicate determinations. This is representative of two experiments.

PLK1 in the checkpoint defective cell lines. The low level of PLK1 in the checkpoint functional cell lines is due to the low expression in interphase cells, few mitotic cells were detected in the wells analysed. This contrasted with the strong staining was observed checkpoint defective lines across the cell cycle, particularly in G2 phase cells (Figure S4). The level of PLK1 staining was increased in the checkpoint functional cell lines with ICRF-193 treatment to levels similar to the checkpoint defective cell line. The increased staining was primarily in G2 phase cells, consistent with the normal increased expression of PLK1 in G2/M phase and the accumulation of G2 phase arrested cells in these cell lines (Figure S4). ICRF-193 treatment had no effect on PLK1 levels in the checkpoint defective lines.

The TCGA melanoma expression data set was interrogated for the level of PLK1 expression in the 468 melanomas with RNAseq data. Initially, the expression levels of PLK1 in samples with mitotic counts were assessed to determine a cut-off for normal expression. Tumours with higher mitotic rates would be expected to have higher PLK1 expression due to the increased proportion of cells in G2/M phase when PLK1 levels are normally increased. There was a poor correlation between mitotic rate and PLK1 levels, but even using a conservative cut-off, there were 11% of melanomas with high levels of PLK1 expression (Figure 4D).

Inhibition of PLK1 restores ATM-dependent checkpoint arrest

The presence of elevated activated PLK1 in checkpoint defective cell lines suggested it may have a role in overcoming the checkpoint arrest. To determine whether the increased PLK1 activity contributed to the inability of ICRF-193-activated ATM signalling to impose a G2 phase delay, the small molecule PLK1 inhibitor BI2536 was used to attempt to re-establish the ICRF-193 imposed delay. PLK1 activity is required for normal G2 phase progression (Lenart et al., 2007), thus concentrations of BI2536 that minimally affected the rate of mitotic entry were determined for each cell line. As previously observed for the checkpoint defective cell lines ((Brooks et al., 2013a) and Figure 1B), the rate of entry into mitosis was not affected by ICRF-193 treatment (Figure 5A, D). However, the combination of ICRF-193 with BI2536 treatment delayed entry into mitosis significantly longer than with BI2536 alone (Figure 5A, D). In the checkpoint functional D28 cell line, the treatment combination of ICRF-193 with BI2536 exacerbated the delay of entry into mitosis caused by ICRF-193 alone, demonstrating that PLK1 is required for exit from the ATM-dependent checkpoint arrest (Figure 5B). PLK1 inhibition failed to re-establish the ICRF-193 dependent G2 delay in the ATM mutant HT144 cells, demonstrating the requirement for active ATM signalling in the checkpoint arrest (Figure 5C). The combination did reduce the rate of entry into mitosis after 12 h, the delayed timing suggesting some effect of this combination on late G1/early S phase cells. When calculated as a percentage of the doubling time of each cell lines, the G2 phase delays obtained with the combined treatment (ICRF+PLK1i) in checkpoint defective cell lines (18, 26 and 21% for D20, SKMel13 and MM415 respectively) were similar to the delays previously observed in the checkpoint functional cell lines [Figure 5E; (Brooks et al., 2013a)].

Over-expression of PLK1 leads to aberrant mitosis

The ability of PLK1 inhibition to restore checkpoint arrest, together with high levels of activated PLK1 in checkpoint defective cells, supports PLK1 dysregulation as the cause of impaired checkpoint arrest. To assess whether over-expression of PLK1 alone was sufficient to bypass the ATM-dependent checkpoint, four ATM-dependent checkpoint functional lines were transduced with a lentivirus expressed wild type myc-PLK1 as an IRES GFP expression construct. In two lines, A2058 and MM603, there was no growth of GFP positive, PLK1 over-expressing clones after 2 months, although GFP positive empty vector cells grew readily. Inspection of transduced cells revealed a 10-fold increase in the number of enlarged multinuclear cells that were also negative for Ki67, suggesting they were senescent (Figure 5A). Both C32 and D28 cells lines produced GFP positive, PLK1 over-expressing populations (Figure S5A), although after sorting for the GFP positive cells, only PLK1 over-expressing C32 cells were able to continuously cultured and uniformly expressed the exogenous myc-PLK1 (Figure 6A). Inspection of C32 cells stably over-expressing PLK1 revealed an accumulation of cells containing micronuclei, compared to the cells expressing GFP alone (Figure 6B, C). These abnormalities further increased following ICRF-193 treatment. Analysis of mitotic figures also revealed a two-fold increase in with anaphase cells with lagging chromosomes, and failed cytokinesis in cells over-

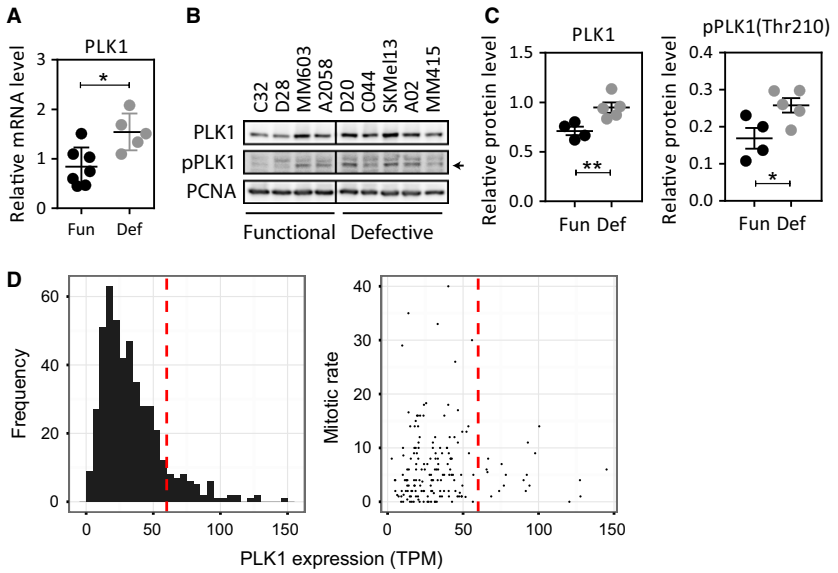

Figure 4. PLK1 level and activity are upregulated in checkpoint defective cell lines. (A) Affymetrix expression data of melanoma cell lines obtained as described in (Johansson et al., 2007). Graphs show group means ± SEM (n = 7 checkpoint functional group, n = 5 checkpoint defective group). Statistical significance values were calculated with unpaired *t*-test; *P<0.05. (B) Cell lysates of five checkpoint functional and five checkpoint defective cell lines were analysed by immunoblotting for PLK1 and pPLK1 and (C) protein levels quantified. Graphs show group means ± SEM (n = 4 checkpoint functional group, n = 5 checkpoint defective group). Statistical significance values were calculated with unpaired *t*-test; *P < 0.05, **P < 0.01. The arrow indicates the pPLK1 band. (D) The TCGA Melanoma database was interrogated for PLK1 expression. The level of PLK1 (measured as transcripts per million (TPM)) was plotted against mitotic rates in the subset of samples with this data to define a conservative cut-off for normal PLK1 expression (red dotted line). Using this cut-off, the whole dataset (468 samples) was plotted.

expressing PLK1 (Figure 6D–G). Few mitotic figures were observed in the ICRF-193 treated GFP controls, whereas they were at least as frequent in the ICRF-193 treated PLK1 over-expressing cells as in either DMSO control-treated lines. The presence of mitotic figures and increased multinuclear cells, both features of mitotic progression with incompletely decatenated chromosomes, demonstrates that PLK1 over-expression was sufficient to overcome the checkpoint arrest imposed by ICRF-193 treatment. ATM-CHK2 activation in these cells was normal (Figure S5B). Loss of the ICRF-193 imposed G2 phase delay was directly demonstrated by time-lapse microscopy, where the PLK1 over-expressing C32 cells displayed no delay of entry into mitosis whereas the vector-transduced controls displayed the expected delay (Figure 6H, I).

Discussion

In this study, we have shown that the defective ATM-dependent checkpoint arrest in melanoma cells is not due to impaired sensing of stimuli or defective ATM signalling, but to an inability to maintain a stable checkpoint arrest. The failure to checkpoint arrest in cells with functional ATM signalling has not previously been reported. Usually, ATM checkpoint defects are due to mutations that result in loss of ATM function, or due to defects in the genes involved in detection or signalling of DNA damage such as BRCA, NBS1 and MRE11 (Lobrich and Jeggo, 2007). ATM checkpoint function has generally been assessed by detection of signalling events, such as activating ATM and CHK2 phosphorylations, or localization of ATM signalling components to DNA damage foci (Bekker-Jensen et al., 2006). Using these criteria, ATM signalling appears to be intact in the melanoma cell lines we investigated, but functional analysis shows the cell lines' ability to checkpoint arrest is clearly defective. We have demonstrated that the basis of this defective checkpoint arrest is dysregulation of PLK1 activity. PLK1 is required for exit from a checkpoint arrest (Van Vugt et al., 2004), and short-term expression of constitutively activated PLK1 has been reported to overcome the ICRF-193 imposed cell cycle arrest (Ando et al., 2013; Deming et al., 2002), suggesting a role for PLK1 in maintaining a stable G2 phase checkpoint arrest. The data presented here demonstrate that in melanomas, ATM signalling and the checkpoint machinery can be intact and functional, but dysregulated PLK1 activity is capable of overcoming the inhibitory ATM-CHK2 signal. This results in failure to stably cell cycle arrest, effectively abrogating the ATM-CHK2 checkpoint function. We have also demonstrated that it is possible to recover this checkpoint arrest by reducing the level of PLK1 activity to tip the balance in favour of the ATM-CHK2 imposed arrest. This finding demonstrates a novel mechanism for abrogating ATM-CHK2 checkpoint function and is the first report of this means of disabling ATM-CHK2 function in a disease setting, in this case melanoma.

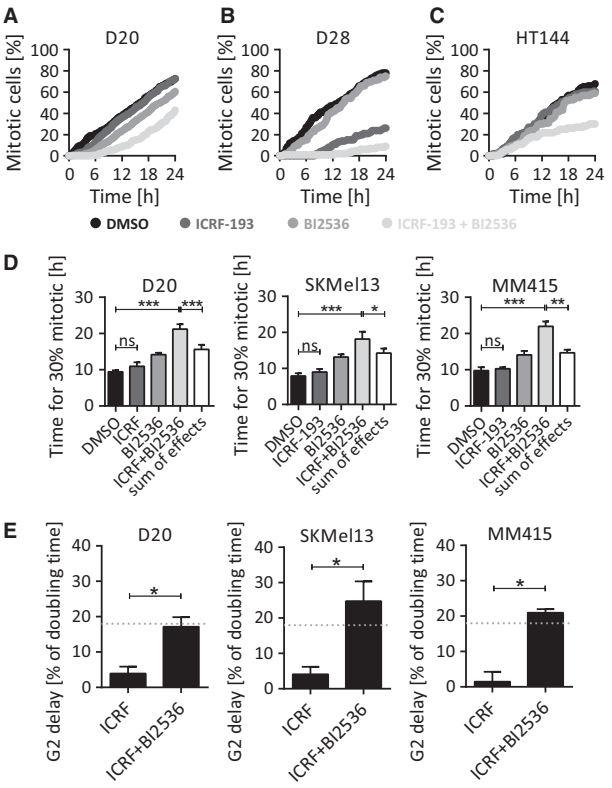

Figure 5. Inhibition of PLK1 restores checkpoint arrest. (A) The checkpoint defective cell line D20 was incubated with 2 μM ICRF-193 and 100 nM BI2536, as single and combination treatments, or with DMSO and the cell rate of entry into mitosis assessed by time-lapse microscopy over a period of 24 h (intervals = 10 min). Graph shows means (n = 3). (B) The same experiment as in (A) was performed with the checkpoint competent cell line D28 and (C) the ATM mutant HT144 cell line. (D) Time extrapolated from experiment depicted in (A) required for 30% of the cell population to enter mitosis. For SKMel13 and MM415, the experiment was performed as for D20 but with 500 and 50 nM BI2536 respectively and repeated n = 5 for MM415. The condition labelled "sum of effects" represents the value obtained by mathematical addition of the values of ICRF-193 and BI2536 single agent effects. Statistical significance values were calculated with one-way ANOVA using Tukey's post hoc test; *P < 0.05, **P < 0.01, ***P < 0.001. (E) G2 delays extrapolated from experiment depicted in (B) and standardized to each cell line's specific doubling time calculated as in (Brooks et al., 2013a). The condition labelled "ICRF+BI2536" represents the value obtained by mathematical subtraction of the BI2536 single agent effect from the effect of ICRF-193 and BI2536 in combination. Grey dotted line = cut-off of decatenation checkpoint defect [18% of doubling time (Brooks et al., 2013a)]. Statistical significance values were calculated with unpaired *t*-test; *P < 0.05.

Mutations of ATM are rare in melanoma. An ATM Ser49Cys substitution associated with increased risk of melanoma has been reported in 10% of melanoma patients in a Danish population study (Dombernowsky et al., 2008). Furthermore, an SNP that encodes an ATM Asp1853Asn substitution has been reported in 13% of melanoma patients and is associated with decreased risk of melanoma (Barrett et al., 2011). The effects of these substitutions on ATM activity are at present unknown, although the Ser49Cys substitution may alter p53 binding (Dombernowsky et al., 2008). Our analysis of ATM activity and localization in response to DNA damage in melanoma cell lines without ATM mutations, did not demonstrate any loss of signalling activity. Additionally, the ability of low doses of PLK1 inhibitor to re-establish the checkpoint arrest indicates that the ATM checkpoint is functional, but it is overcome by the elevated PLK1. Recently, a meta-analysis of GWAS studies identified a SNP in ATM as one of the strongest links with melanoma development (Law et al., 2015). ATM is normally associated with double strand break repair, whereas melanoma is more usually associated with single-stranded DNA damage caused by UV radiation and involving ATR-CHK1 signalling (Pavey et al., 2013; Wigan et al., 2012). Together with the novel defect in ATM checkpoint function identified in this work, this provides strong evidence for a previously unappreciated role for ATM in the development of melanoma.

The fundamental difference between the novel defect in the ATM-dependent checkpoint we identified and inactivating (usually truncating) ATM mutations is highlighted by the distinct phenotypes these defects confer to cells in response to DNA insult. ATM mutant cells, which have loss of ATM signalling and function, are hypersensitive to agents that promote DSBs (Huo et al., 1994). By contrast, we have found that ATM checkpoint defective melanoma cell lines have similar sensitivity to DSBs as the checkpoint functional lines. The HT144 melanoma cell line, which has a truncating mutation of ATM (Ramsay et al., 1998), demonstrated the expected hypersensitivity to DSB agents. This indicates the ability of ATM to protect cells from DSB insult is intact although the checkpoint arrest is lost. Disruption of the ATM-dependent checkpoint response through dysregulated PLK1 may also contribute to the cancer development. The loss of the checkpoint arrest would result in cells failing to appropriately arrest to allow time for complete repair of DNA damage, and because checkpoint signalling remains intact, cancer cells have the benefit of active ATM-dependent anti-apoptotic signalling to promote survival. The increased proportion of cells with micronuclei we observed in the PLK1 over-expressing C32 cells demonstrates the effectiveness of this mechanism to promote genomic instability.

The ability of elevated levels of PLK1 to bypass the ATM checkpoint suggests dysregulation of PLK1 expression and/or activity might be a common feature of melanomas. Although no genetic alterations in the PLK1 locus have been reported in melanomas, the TCGA expression data indicates that conservatively, 11% of melanomas have increased PLK1 expression, and this has also been observed at the protein level in primary and metastatic melanomas (Jalili et al., 2011; Strebhardt et al., 2000). In an earlier study, we identified PLK1 as a gene that was significantly downregulated in the decatenation checkpoint defective melanoma cell lines (Brooks et al., 2013a). Another study also examining G2 phase checkpoint defective melanomas cell lines failed to detect

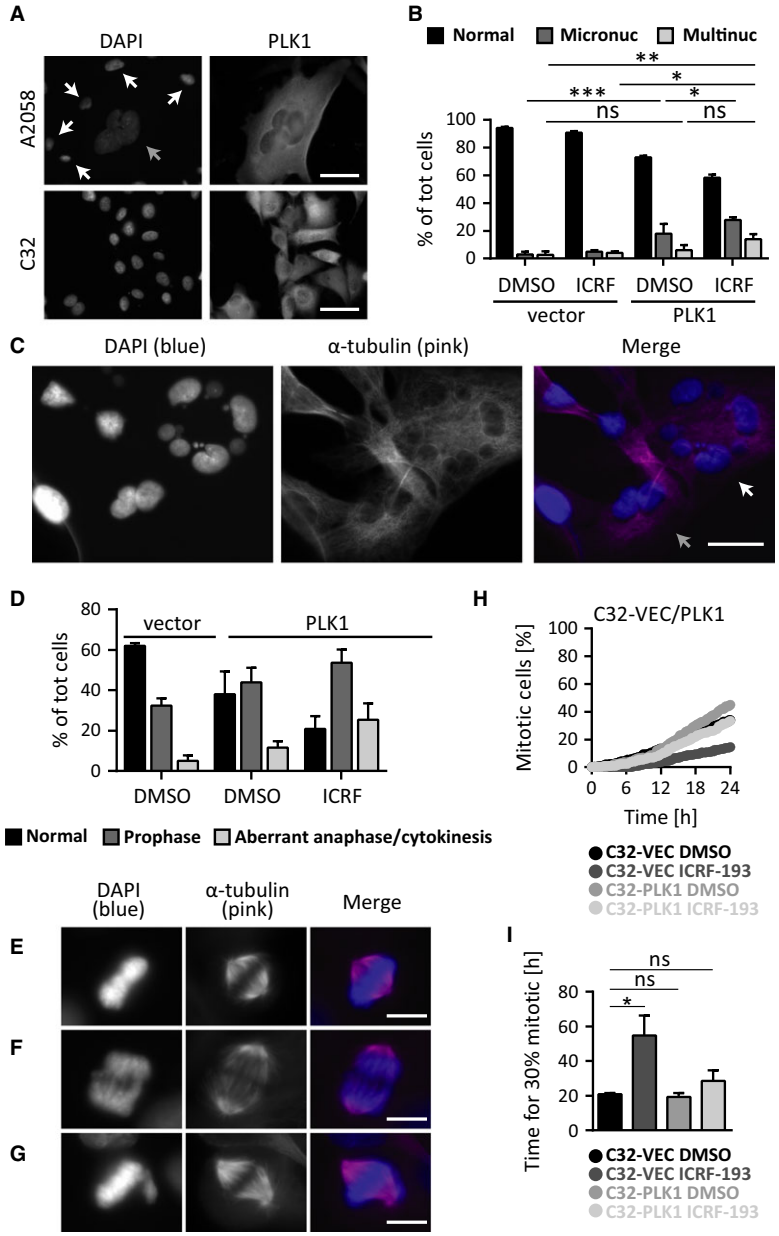

Figure 6. Over-expression of PLK1 leads to aberrant mitosis. (A) Immunofluorescence microscopy of A2058 and C32 checkpoint functional cell lines stably transduced with human PLK1 gene and stained using DAPI and PLK1 antibody. Scale bar = 50 μm. White arrows indicate normal size cells with undetectable levels of PLK1. The grey arrow indicates an abnormally large cell expressing high levels of PLK1. (B) Frequency quantification of abnormal nuclear structures in C32 cells stably over-expressing PLK1 under normal conditions (DMSO) and following 2 μM ICRF-193 treatment for 24 h. Cells were stained with DAPI and α-tubulin antibody and nuclear structures identified by immunofluorescence microscopy. A minimum of at least 100 cells were analysed per condition, and the experiment was performed in triplicate. "Normal" = cells with normal nucleus; micronuc = cells with micronuclei; multinuc = cells with multiple nuclei. (C) Samples of immunofluorescence images used for the quantification described in (C) showing two multinucleate cells (white and grey arrows), one of which with micronuclei (white arrow). Scale bar = 30 μm. (D) Frequency of abnormal prophases and anaphases quantified from the experiment described in (C). Normal = cells with normal prophase and anaphase. A minimum of at least 100 cells were analysed per condition, and the experiment performed in triplicate. Data for the empty vector expressing cells treated with ICRF-193 were omitted due to low numbers of mitotic cells available for this condition. (E–G) Representative immunofluorescence images from the experiment described in (C) showing a cell undergoing normal mitosis (E), anaphase cell with lagging chromosomes (aberrant anaphase) (F) and metaphase cells with failure of congression (prophase) (G). Scale bar = 10 μm. (H) The C32 vector only transduced (C32-VEC) and PLK1 over-expressing (C32-PLK1) cell lines were treated with either DMSO or 2 μM ICRF-193 and followed by time-lapse microscopy as in Figure 1. The data are the mean of replicate experiments (n = 3). (I) Time extrapolated from experiment depicted in (H) required for 30% of the cell population to enter mitosis. For SKMel13 and MM415, the experiment was performed as for D20 but with 500 and 50 nM BI2536 respectively and repeated n = 5 for MM415. Statistical significance values were calculated with one-way ANOVA using Tukey's post hoc test; *P < 0.05, **P < 0.01, ***P < 0.001, ns = P > 0.05.

PLK1 in a similar transcriptomic analysis (Omolo et al., 2013). This may be due to the use of ionizing radiation to trigger the checkpoint response, which utilizes both ATM and ATR signalling rather than ATM alone in the case of ICRF193 used here. Elevated Aurora A kinase activity, an upstream regulator of PLK1 (Seki et al., 2008), has been linked to mutations in protein phosphatase 6 (PP6) that regulates Aurora A activity (Hammond et al., 2013). PP6 mutations are found in approximately 10% of melanomas (Hodis et al., 2012; Krauthammer et al., 2012; Stark et al., 2012). Thus elevated Aurora A activity and increased PLK1 expression are likely to contribute to the elevated PLK1 activity we have observed. The use of PLK1 inhibitors in melanomas has been reported (Schmit et al., 2009). The mitotic catastrophe and apoptosis produced by inhibition of PLK1 are independent of the level of PLK1 expression.

In conclusion, we have characterized a novel defect of the ATM-dependent cell cycle checkpoint that is not caused by ATM inactivating mutations, but is instead due to an inability of cells to stably checkpoint arrest in response to ATM-dependent signalling. This is a consequence of dysregulation of PLK1, which drives the cells prematurely from the checkpoint arrest, promoting genomic instability.

Methods

Cell lines and culturing conditions

All human melanoma cell lines (A2058, A02, C32, C044, D20, D22, D28-M3, MM415, MM603 and SKMel13) were provided by Dr Nick Hayward (Queensland Institute of Medical Research-Berghofer) and grown as previously described (Brooks et al., 2013a). All cell lines were confirmed to be mycoplasma free and their identity confirmed by Short Tandem Repeats (STR) fingerprinting at Queensland Institute of Medical Research-Berghofer within 6 months of the experiments being performed.

Time-lapse microscopy

Cells were seeded in multiwell plates, and time-lapse microscopy was performed using a Zeiss Axiovert 200M Cell Observer (North Ryde, Australia) equipped with an incubation chamber at 37°C and 5% CO_2 as described previously (Brooks et al., 2013a). Images were taken at intervals of 10–15 min. Cells were treated with 2 μM ICRF-193 (Biomol, Waterloo, Australia), 2 μM etoposide (Sigma), 40 μg/ml phleomycin (Sigma, Castle Hill, Australia), or equivalent DMSO volumes. Cell morphology was monitored to observe entry into mitosis and time required to enter mitosis recorded. Images were analysed using a minimum of 100 cells per cell line and per treatment. The G2 phase delay was calculated as explained in (Brooks et al., 2013a).

Immunoblotting

Cell pellets were lysed and prepared for immunoblotting as previously (Brooks et al., 2013a). Lysates were equalized for protein content then separated by SDS-PAGE and transferred to nitrocellulose membranes. Membranes were probed with antibodies against human Bora, phospho-ATM Ser1981, phospho-CHK1 Ser317, phospho-CHK2 Thr68, phospho-PLK1 Thr210 (Cell Signalling, Arundel, Australia; #12109, #4526, #2344, #2661, #9062), α-actin (Sigma), α-tubulin (Abcam, Waterloo, Australia; #ab18251), Aurora A (BD Biosciences, North Ryde, Australia; #610938), PCNA (Dako, North Sydney, Australia; #M0879), PLK1 (Calbiochem, Frenchs Forest, Australia; #DR1037). Proteins were visualized using chemiluminescence detection. Protein levels were quantified using IMAGEJ software (http://rsbweb.nih.gov/ij/).

Immunofluorescence

Cells were grown on poly-L-lysine-coated glass coverslips and treated with 2 μM ICRF-193, 2 μM etoposide, 40 μg/ml phleomycin, or equivalent DMSO volumes for 6 h. Cells were fixed-permeabilized in cold methanol and immunostained with antibodies against human phospho-ATM Ser1981 (Cell Signalling #4526), phospho-H2AX Ser139 (Millipore, Bayswater, Australia; #07-164), α-tubulin (Sigma #T6199), 53BP1 (BD Biosciences #612522), 4′,6-diamidino-2-phenylindole (DAPI) DNA stain, and appropriate secondary antibodies.

PLK1 over-expression in melanoma cell lines

The lentiviral expression clone PLK1-pLV411G was generated using the Gateway® Technology (Invitrogen) according to the manufacturer's instructions. Briefly, *att*B sites were generated by PCR on the N-terminally myc-tagged PLK1 cDNA and the resulting product cloned into the pDONR221 donor vector by the BP reaction generating the entry clone. The resulting cloned gene was then subcloned into the pLV411G destination vector by the LR reaction between the entry clone and the destination vector. Lentivirus supernatant was generated by co-transfection of HEK293FT cells with the construct of interest and the packaging mix (Invitrogen, Scoresby, Australia) using Lipofectamine 2000TM (Invitrogen). Melanoma cell lines were transduced by 2.5 h incubation with the lentivirus supernatant, then sorted by FACS according to their GFP signal.

High content imaging

Cells were seeded in clear-bottom 96-well Viewplates (PerkinElmer, Glen Waverley, Australia) for 2 days then fixed-permeabilized in cold methanol and immunostained with appropriate antibodies. Images were acquired with a Cellomics ArrayScan VTI (Thermo Scientific, Waltham, MA, USA) high content imager, and analysed as reported previously (Brooks et al., 2013b). The images and data were exported to R software for statistical analysis.

Acknowledgements

The University of Queensland is a shareholder in the Translational Research Institute (TRI) which is supported by a grant from the Australian Government; and funding from the Queensland Government, Atlantic Philanthropies, Queensland University of Technology and The University of Queensland. Melanoma cell lines were originally sourced from Chris Schmidt and a subset is available from the Australasian Biospecimen Network (Oncology). Thanks to Nick Hayward for making the mutation data available. This work was supported by grants from Cancer Council Queensland and the National Health and Medical Research Council of Australia (NHMRC; Grant ID 1029260) and Worldwide Cancer Research (formerly Association for International Cancer Research). BG is an NHMRC Senior Research Fellow. The authors thank Drs Pascal Duijf, Martin Lavin and Fiona McMillan for their critical reading of this manuscript.

Author contributions

LS and KB devised, performed and oversaw experiments, analysed data and contributed to writing the manuscript.

KNC, GG, MD-H, DS performed experiments and analysed data, JE analysed the TCGA data, BB provided analysis and discussion, BG designed and supervised experimental plan, analysed data and wrote the manuscript.

Conflict of interest

The authors have no conflict of interests to declare.

References

Ando, K., Ozaki, T., Hirota, T., and Nakagawara, A. (2013). NFBD1/MDC1 is phosphorylated by PLK1 and controls G2/M transition through the regulation of a TOPOIIalpha-mediated decatenation checkpoint. PLoS ONE *8*, e82744.

Barrett, J.H., Iles, M.M., Harland, M. et al. (2011). Genome-wide association study identifies three new melanoma susceptibility loci. Nat. Genet. *43*, 1108–1113.

Bartek, J., Lukas, C., and Lukas, J. (2004). Checking on DNA damage in S phase. Nat. Rev. Mol. Cell Biol. *5*, 792–804.

Bekker-Jensen, S., Lukas, C., Kitagawa, R., Melander, F., Kastan, M.B., Bartek, J., and Lukas, J. (2006). Spatial organization of the mammalian genome surveillance machinery in response to DNA strand breaks. J. Cell Biol. *173*, 195–206.

Boutros, R., Dozier, C., and Ducommun, B. (2006). The when and wheres of CDC25 phosphatases. Curr. Opin. Cell Biol. *18*, 185–191.

Bower, J.J., Zhou, Y., Zhou, T., Simpson, D.A., Arlander, S.J., Paules, R.S., Cordeiro-Stone, M., and Kaufmann, W.K. (2010). Revised genetic requirements for the decatenation G(2) checkpoint: the role of ATM. Cell Cycle *9*, 1617–1628.

Brooks, K., Chia, K.M., Spoerri, L., Mukhopadhyay, P., Wigan, M., Stark, M., Pavey, S., and Gabrielli, B. (2013a). Defective decatenation checkpoint function is a common feature of melanoma. J. Invest. Dermatol. *134*, 150–159.

Brooks, K., Oakes, V., Edwards, B. et al. (2013b). A potent Chk1 inhibitor is selectively cytotoxic in melanomas with high levels of replicative stress. Oncogene *32*, 788–796.

Deming, P.B., Flores, K.G., Downes, C.S., Paules, R.S., and Kaufmann, W.K. (2002). ATR enforces the topoisomerase II-dependent G2 checkpoint through inhibition of Plk1 kinase. J. Biol. Chem. *277*, 36832–36838.

Doherty, S.C., Mckeown, S.R., Mckelvey-Martin, V., Downes, C.S., Atala, A., Yoo, J.J., Simpson, D.A., and Kaufmann, W.K. (2003). Cell cycle checkpoint function in bladder cancer. J. Natl Cancer Inst. *95*, 1859–1868.

Dombernowsky, S.L., Weischer, M., Allin, K.H., Bojesen, S.E., Tybjaerg-Hansen, A., and Nordestgaard, B.G. (2008). Risk of cancer by ATM missense mutations in the general population. J. Clin. Oncol. *26*, 3057–3062.

Hammond, D., Zeng, K., Espert, A., Bastos, R.N., Baron, R.D., Gruneberg, U., and Barr, F.A. (2013). Melanoma-associated mutations in protein phosphatase 6 cause chromosome instability and DNA damage owing to dysregulated Aurora-A. J. Cell Sci. *126*, 3429–3440.

Hill, V.K., Gartner, J.J., Samuels, Y., and Goldstein, A.M. (2013). The genetics of melanoma: recent advances. Annu. Rev. Genomics Hum. Genet. *14*, 257–279.

Hodis, E., Watson, I.R., Kryukov, G.V. et al. (2012). A landscape of driver mutations in melanoma. Cell *150*, 251–263.

Huo, Y.K., Wang, Z., Hong, J.H., Chessa, L., Mcbride, W.H., Perlman, S.L., and Gatti, R.A. (1994). Radiosensitivity of ataxia-telangiectasia, X-linked agammaglobulinemia, and related syndromes using a modified colony survival assay. Cancer Res. *54*, 2544–2547.

Jalili, A., Moser, A., Pashenkov, M., Wagner, C., Pathria, G., Borgdorff, V., Gschaider, M., Stingl, G., Ramaswamy, S., and Wagner, S.N. (2011). Polo-like kinase 1 is a potential therapeutic target in human melanoma. J. Invest. Dermatol. *131*, 1886–1895.

Johansson, P., Pavey, S., and Hayward, N. (2007). Confirmation of a BRAF mutation-associated gene expression signature in melanoma. Pigment Cell Res. *20*, 216–221.

Kaufmann, W.K., Nevis, K.R., Qu, P. et al. (2008). Defective cell cycle checkpoint functions in melanoma are associated with altered patterns of gene expression. J. Invest. Dermatol. *128*, 175–187.

Kaufmann, W.K., Carson, C.C., Omolo, B., Filgo, A.J., Sambade, M.J., Simpson, D.A., Shields, J.M., Ibrahim, J.G., and Thomas, N.E. (2014). Mechanisms of chromosomal instability in melanoma. Environ. Mol. Mutagen. *55*, 457–471.

Krauthammer, M., Kong, Y., Ha, B.H. et al. (2012). Exome sequencing identifies recurrent somatic RAC1 mutations in melanoma. Nat. Genet. *44*, 1006–1014.

Law, M.H., Bishop, D.T., Lee, J.E. et al. (2015). Genome-wide meta-analysis identifies five new susceptibility loci for cutaneous malignant melanoma. Nat. Genet. *47*, 987–995.

Lenart, P., Petronczki, M., Steegmaier, M., Di Fiore, B., Lipp, J.J., Hoffmann, M., Rettig, W.J., Kraut, N., and Peters, J.M. (2007). The small-molecule inhibitor BI 2536 reveals novel insights into mitotic roles of polo-like kinase 1. Curr. Biol. *17*, 304–315.

Lobrich, M., and Jeggo, P.A. (2007). The impact of a negligent G2/M checkpoint on genomic instability and cancer induction. Nat. Rev. Cancer *7*, 861–869.

Lu, M., Miller, P., and Lu, X. (2014). Restoring the tumour suppressive function of p53 as a parallel strategy in melanoma therapy. FEBS Lett. *588*, 2616–2621.

Luo, K., Yuan, J., Chen, J., and Lou, Z. (2009). Topoisomerase IIalpha controls the decatenation checkpoint. Nat. Cell Biol. *11*, 204–210.

Macurek, L., Lindqvist, A., Lim, D., Lampson, M.A., Klompmaker, R., Freire, R., Clouin, C., Taylor, S.S., Yaffe, M.B., and Medema, R.H. (2008). Polo-like kinase-1 is activated by aurora A to promote checkpoint recovery. Nature *455*, 119–123.

Medema, R.H., and Macurek, L. (2012). Checkpoint control and cancer. Oncogene *31*, 2601–2613.

Nakagawa, T., Hayashita, Y., Maeno, K., Masuda, A., Sugito, N., Osada, H., Yanagisawa, K., Ebi, H., Shimokata, K., and Takahashi, T. (2004). Identification of decatenation G2 checkpoint impairment independently of DNA damage G2 checkpoint in human lung cancer cell lines. Cancer Res. *64*, 4826–4832.

Omolo, B., Carson, C., Chu, H., Zhou, Y., Simpson, D.A., Hesse, J.E., Paules, R.S., Nyhan, K.C., Ibrahim, J.G., and Kaufmann, W.K. (2013). A prognostic signature of G 2 checkpoint function in melanoma cell lines. Cell Cycle *12*, 1071–1082.

Pavey, S., Spoerri, L., Haass, N.K., and Gabrielli, B. (2013). DNA repair and cell cycle checkpoint defects as drivers and therapeutic targets in melanoma. Pigment Cell Melanoma Res. *10*, 12136.

Ramsay, J., Birrell, G., Baumann, K., Bodero, A., Parsons, P., and Lavin, M. (1998). Radiosensitive melanoma cell line with mutation of the gene for ataxia telangiectasia. Br. J. Cancer *77*, 11–14.

Schmit, T.L., Zhong, W., Setaluri, V., Spiegelman, V.S., and Ahmad, N. (2009). Targeted depletion of Polo-like kinase (Plk) 1 through lentiviral shRNA or a small-molecule inhibitor causes mitotic catastrophe and induction of apoptosis in human melanoma cells. J. Invest. Dermatol. *129*, 2843–2853.

Seki, A., Coppinger, J.A., Jang, C.Y., Yates, J.R., and Fang, G. (2008). Bora and the kinase Aurora a cooperatively activate the kinase Plk1 and control mitotic entry. Science *320*, 1655–1658.

Smits, V.A., Klompmaker, R., Arnaud, L., Rijksen, G., Nigg, E.A., and Medema, R.H. (2000). Polo-like kinase-1 is a target of the DNA damage checkpoint. Nat. Cell Biol. *2*, 672–676.

Stark, M.S., Woods, S.L., Gartside, M.G. et al. (2012). Frequent somatic mutations in MAP3K5 and MAP3K9 in metastatic melanoma identified by exome sequencing. Nat. Genet. *44*, 165–169.

Strebhardt, K., Kneisel, L., Linhart, C., Bernd, A., and Kaufmann, R. (2000). Prognostic value of pololike kinase expression in melanomas. JAMA *283*, 479–480.

Tsvetkov, L., and Stern, D.F. (2005). Phosphorylation of Plk1 at S137 and T210 is inhibited in response to DNA damage. Cell Cycle *4*, 166–171.

Van Vugt, M.A., Bras, A., and Medema, R.H. (2004). Polo-like kinase-1 controls recovery from a G2 DNA damage-induced arrest in mammalian cells. Mol. Cell *15*, 799–811.

Wigan, M., Pinder, A., Giles, N., Pavey, S., Burgess, A., Wong, S., Sturm, R., and Gabrielli, B. (2012). A UVR-induced G2 phase checkpoint response to ssDNA gaps produced by replication fork bypass of unrepaired lesions is defective in melanoma. J. Invest. Dermatol. *132*, 1681–1688.

Supporting information

Additional Supporting Information may be found in the online version of this article:

Figure S1. Lack of ATR-CHK1 activation with ICRF-193 treatment.

Figure S2. Supplementary data on pCHK2 and pATM levels.

Figure S3. Localisation of ATM checkpoint signalling components.

Figure S4. Quantitative cell analysis of PLK1 immunofluorescence signal.

Figure S5. PLK1 over-expression and ATM-CHK2 activation.

Table S1. Mutation status of p53, BRAF, CDK4 and Nras for each of the cell lines indicated are shown.